Virial expansion around the *s*-wave Feshbach resonance in mass-imbalanced Fermi gases

Ting Xie, Xue-Jin Hu, Yin Huang, Gao-Ren Wang, and Shu-Lin Cong*
School of Physics and Optoelectronic Technology, Dalian University of Technology, Dalian 116024, China
(Received 12 January 2014; published 11 March 2014)

We derive the expressions for the virial coefficients up to the third order for two-species fermion mixtures, and investigate the fugacity of the species and the interaction energy density around the *s*-wave Feshbach resonance in ^{6}Li-^{40}K mixtures. The theoretical results show that the magnitude of the virial coefficients depends on the mass ratio in a mass-imbalanced system. We find that the contribution of two-body bound states to high-order virial coefficients is very small at temperatures of microkelvin order. With the decrease of T/T_F, the positions of the maxima of fugacity and interaction energy density shift away from the resonance position in the third-order virial expansion calculation. The mass ratio determines the relevance between the fugacity and number density of heavy species. Our conclusion is also effective for other mass-imbalanced systems.

DOI: 10.1103/PhysRevA.89.032704 PACS number(s): 34.50.Cx, 67.85.−d

I. INTRODUCTION

Feshbach resonances play an important role in the study of ultracold atomic gases since they offer exceptional control over the interatomic interactions at low temperature [1]. In the vicinity of a Feshbach resonance, the interaction between species becomes significant and a weakly bound two-body state forms. Due to their collisional stability, strongly interacting Fermi systems are often the source of macroscopic effects.

In the past few years, numerous theories and experiments on strongly interacting Fermi systems have aimed at two-component spin mixtures of identical fermion species [2–4]. Recently, the study of two-species Fermi gases has attracted considerable interest from researchers [5–10] . Compared with single fermion species, unequal masses can lead to very rich phase diagrams and novel few-body phenomena [11,12]. As a strongly interacting Fermi-Fermi system, the combination of Li and K has been investigated by many groups in experiments [5–7,10]. In particular, Grimm and co-workers measured the complete excitation spectrum of ^{40}K impurities immersed in a ^{6}Li Fermi sea in the vicinity of a wide Feshbach resonance at $T = 0.16\varepsilon_F$, where ε_F is the effective Fermi energy [10]. The existence of a long-lived, metastable many-body state offers intriguing prospects for the creation of exotic quantum phases in ultracold, repulsively interacting Fermi gases.

The development of experimental techniques has inspired theoretical researchers to develop various approaches to research the quantum behavior of ultracold atomic gases [13–19] . The quantum virial expansion is an effective method to study the phenomena associated with the spin degree of freedom [15–18]. This method was proposed by Beth and Uhlenbeck to investigate the few-body problem [20]. Then Lee and Yang suggested that the cluster function of Bose-Einstein or Fermi-Dirac gases can be related to the corresponding function of a Boltzmann system, and the complex *N*-body problem can be reduced to a two-body system using the binary collision method [21]. However, this theory has not been applied to mass-imbalanced Fermi gases.

Liu *et al*. investigated the high-temperature properties of a strongly correlated Fermi gas for a spin-imbalanced Fermi mixture using the virial expansion method [22]. In this paper, we investigate theoretically the thermodynamics near an *s*-wave Feshbach resonance in ^{6}Li-^{40}K Fermi gases based on Lee-Yang theory. The paper is organized as follows. In Sec. II, we present the virial expansion for a mass-imbalanced Fermi gas, and derive the interaction energy density for varying fugacity in a magnetic field. In Sec. III, the calculated results for the virial coefficients, fugacity, and interaction energy are given and discussed. Finally, a conclusion is drawn in Sec. IV.

II. QUANTUM VIRIAL EXPANSION FOR MASS-IMBALANCED FERMI GASES

To apply the quantum virial expansion theory, the fugacity $z = \exp(\mu/k_BT) \ll 1$ is required. We can expand the thermodynamic potential Ω in powers of z with a small error. For the two-species fermion mixture composed of N_1 particles γ_1 and N_2 particles γ_2, the Hamiltonian can be written as

$$\hat{H}^{\mathrm{FD}}_{N_1,N_2} = -\frac{\hbar^2}{2m_1}\sum_{i=1}^{N_1}\nabla_i^2 - \frac{\hbar^2}{2m_2}\sum_{j=1}^{N_2}\nabla_j^2 + \sum_{i<j}u(\mathbf{r}_{ij}), \quad (1)$$

where m_1 is the mass of species γ_1 and m_2 the mass of species γ_2. $\mathbf{r}_{ij}$ and $u(\mathbf{r}_{ij})$ denote the relative coordinate of the two particles and the interaction energy, respectively. The superscript "FD" represents the Fermi-Dirac gas. Three- and more-particle interactions are not considered here. The thermodynamic potential of the two-component Fermi gas in the grand canonical ensemble is given by

$$\Omega = -k_BT\ln\mathrm{Tr}\exp\left[-\left(H^{\mathrm{FD}}_{N_1,N_2} - \mu_1N_1 - \mu_2N_2\right)/(k_BT)\right], \quad (2)$$

where T is the temperature of the system and μ_i the chemical potential of species γ_i.

Taylor expanding Eq. (2) to the third order [22], we obtain

$$\Omega = -k_BT\frac{V}{\lambda_{m_1}^3}\sum_{N_1=1}^{\infty}b_{N_1,0}z_1^{N_1} - k_BT\frac{V}{\lambda_{m_1}^3}\sum_{N_2=1}^{\infty}b_{0,N_2}z_2^{N_2} - k_BT\frac{V}{\lambda_{m_1}^3}\sum_{N_1=1}^{\infty}\sum_{N_2=1}^{\infty}b_{N_1,N_2}z_1^{N_1}z_2^{N_2}, \quad (3)$$

*shlcong@dlut.edu.cn

where k_B is the Boltzmann constant, V the volume, and $\lambda_{m_1} = h/\sqrt{2\pi m_1 k_B T}$ the thermal wavelength of species γ_1. The expansion coefficient $V/\lambda_{m_1}^3$ is not unique. Its variation will change the magnitude of the virial coefficient to different extents. However, it does not change the thermodynamic potential and the interaction energy. To simplify the calculation, we use the same expansion coefficient $V/\lambda_{m_1}^3$ for all virial coefficients in the present work. The N_1th (N_2th) virial coefficient $b_{N_1,0}$ (b_{0,N_2}) arises from the interaction in the single species γ_1 (γ_2). The third term with b_{N_1,N_2} in Eq. (3) describes the interaction between distinguishable species. In this paper, we define b_{N_1,N_2} as the (N_1+N_2)th virial coefficient.

We introduce the operator

$$W^{\mathrm{FD}}_{N_1,N_2} = \exp\left(-\frac{H^{\mathrm{FD}}_{N_1,N_2}}{k_B T}\right), \tag{4}$$

whose matrix element in coordinate representation is given by

$$\begin{aligned}
&\langle 1',\ldots N_1',(N_1+1)',\ldots,(N_1+N_2)'| \\
&\quad\times W^{\mathrm{FD}}_{N_1,N_2}|1,\ldots,N_1,N_1+1,\ldots,N_1+N_2\rangle \\
&= N_1!N_2!\sum_{i,\mathrm{symm}}\psi_i(1',2',\ldots,N')\psi_i^*(1,2,\ldots,N) \\
&\quad\times\exp\left(\frac{-E_i}{k_B T}\right),
\end{aligned} \tag{5}$$

where $1,2,\ldots,N_1$ denote the coordinates of species γ_1 and $N_1+1,N_1+2,\ldots,N_1+N_2$ the coordinates of species γ_2 in space. ψ_i and E_i are the normalized eigenfunction and eigenvalue of $\hat{H}^{\mathrm{FD}}_{N_1,N_2}$, respectively. The partition function is given by

$$\begin{aligned}
Q_{N_1,N_2} &\equiv \mathrm{Tr}\left[\exp\left(\frac{-H^{\mathrm{FD}}_{N_1,N_2}}{k_B T}\right)\right] \\
&= \int\langle 1',2',\ldots,(N_1+N_2)'|W^{\mathrm{FD}}_{N_1,N_2}|1,2,\ldots,N_1+N_2\rangle \\
&\quad\times d^3 r.
\end{aligned} \tag{6}$$

The cluster functions U_{N_1,N_2} are defined as

$$W^{\mathrm{FD}}_{1,0}(1) = U^{\mathrm{FD}}_{1,0}(1) = \frac{1}{\lambda^3_{m_1}}, \tag{7a}$$

$$W^{\mathrm{FD}}_{0,1}(1) = U^{\mathrm{FD}}_{0,1}(1) = \frac{1}{\lambda^3_{m_2}}, \tag{7b}$$

$$W^{\mathrm{FD}}_{1,1}(1,2) = U^{\mathrm{FD}}_{1,0}(1)U^{\mathrm{FD}}_{0,1}(2) + U^{\mathrm{FD}}_{1,1}(1,2), \tag{7c}$$

$$W^{\mathrm{FD}}_{2,0}(1,2) = U^{\mathrm{FD}}_{1,0}(1)U^{\mathrm{FD}}_{1,0}(2) + U^{\mathrm{FD}}_{2,0}(1,2), \tag{7d}$$

$$W^{\mathrm{FD}}_{0,2}(1,2) = U^{\mathrm{FD}}_{0,1}(1)U^{\mathrm{FD}}_{0,1}(2) + U^{\mathrm{FD}}_{0,2}(1,2), \tag{7e}$$

$$\begin{aligned}
W^{\mathrm{FD}}_{3,0}(1,2,3) &= U^{\mathrm{FD}}_{1,0}(1)U^{\mathrm{FD}}_{1,0}(2)U^{\mathrm{FD}}_{1,0}(3) + U^{\mathrm{FD}}_{1,0}(1)U^{\mathrm{FD}}_{2,0}(2,3) \\
&\quad + U^{\mathrm{FD}}_{1,0}(2)U^{\mathrm{FD}}_{2,0}(3,1) + U^{\mathrm{FD}}_{1,0}(3)U^{\mathrm{FD}}_{2,0}(1,2) \\
&\quad + U^{\mathrm{FD}}_{3,0}(1,2,3),
\end{aligned} \tag{7f}$$

$$\begin{aligned}
W^{\mathrm{FD}}_{2,1}(1,2,3) &= U^{\mathrm{FD}}_{1,0}(1)U^{\mathrm{FD}}_{1,0}(2)U^{\mathrm{FD}}_{0,1}(3) + U^{\mathrm{FD}}_{1,0}(1)U^{\mathrm{FD}}_{1,1}(2,3) \\
&\quad + U^{\mathrm{FD}}_{1,0}(2)U^{\mathrm{FD}}_{1,1}(3,1) + U^{\mathrm{FD}}_{0,1}(3)U^{\mathrm{FD}}_{2,0}(1,2) \\
&\quad + U^{\mathrm{FD}}_{2,1}(1,2,3),
\end{aligned} \tag{7g}$$

$$\vdots$$

where λ_{m_2} is the thermal wavelength of species γ_2. The virial coefficient can be expressed in $U^{\mathrm{FD}}_{N_1,N_2}$ as [21]

$$b_{N_1,N_2} = \frac{\lambda^3_{m_1}}{N_1!N_2!V}\mathrm{Tr}\left(U^{\mathrm{FD}}_{N_1,N_2}\right). \tag{8}$$

A. Second virial coefficients

According to Eq. (3), the second virial coefficient contains three components, $b_{2,0}$, $b_{0,2}$, and $b_{1,1}$. The expression for $b_{2,0}$ or $b_{0,2}$ can be found in the theory of Mayer and co-workers [23–26]. In the following, we give only the expression of $b_{1,1}$.

The two-body Hamiltonian reads

$$\hat{H}^{\mathrm{FD}}_{1,1} = -\frac{\hbar^2}{2m_1}\nabla^2 - \frac{\hbar^2}{2m_2}\nabla^2 + u(|\mathbf{r}_1-\mathbf{r}_2|), \tag{9}$$

where $\mathbf{r}_1$ ($\mathbf{r}_2$) is the coordinate of particle 1 (2). The center-of-mass coordinate $\mathbf{R}$ and relative coordinate $\mathbf{r}$ are given by

$$\mathbf{R} = (m_1\mathbf{r}_1 + m_2\mathbf{r}_2)/(m_1+m_2), \tag{10}$$

$$\mathbf{r} = \mathbf{r}_2 - \mathbf{r}_1. \tag{11}$$

The eigenfunctions and eigenvalues of $\hat{H}^{\mathrm{FD}}_{1,1}$ can be written as

$$\psi_\alpha(1,2) = \psi_\alpha(\mathbf{R},\mathbf{r}) = \frac{1}{\sqrt{V}}\exp[(i(\mathbf{P}_j\cdot\mathbf{R})/\hbar)]\varphi_n(\mathbf{r}), \tag{12}$$

$$E_\alpha = \frac{P_j^2}{2(m_1+m_2)} + \varepsilon_n, \tag{13}$$

where P_j is the momentum of two particles, and $\alpha = (j,n)$. φ_n and ε_n satisfy the Schrödinger equation

$$\left\{-\frac{\hbar^2}{2m_r}\nabla_r^2 + u(\mathbf{r})\right\}\varphi_n(\mathbf{r}) = \varepsilon_n(\mathbf{r}), \tag{14}$$

where m_r is the reduced mass of two particles.

Substituting Eqs. (9)–(14) into Eq. (8), we get

$$\begin{aligned}
b_{1,1} &= \frac{\lambda^3_{m_1}}{V}\sum_\alpha\left[\exp\left(-\frac{E_\alpha}{k_B T}\right) - \exp\left(-\frac{E^0_\alpha}{k_B T}\right)\right] \\
&= \frac{\lambda^3_{m_1}}{V}\sum_j\exp\left[\frac{-P_j^2}{2(m_1+m_2)k_B T}\right] \\
&\quad\times\sum_n\left[\exp\left(-\frac{\varepsilon_n}{k_B T}\right) - \exp\left(-\frac{\varepsilon^0_n}{k_B T}\right)\right] \\
&= 2\sqrt{2}\frac{\lambda^3_{m_1}}{\lambda^3_{M/2}}\sum_n\left[\exp\left(-\frac{\varepsilon_n}{k_B T}\right) - \exp\left(-\frac{\varepsilon^0_n}{k_B T}\right)\right].
\end{aligned} \tag{15}$$

The superscript 0 denotes the noninteracting contribution and $\lambda_{M/2} = h/\sqrt{\pi(m_1+m_2)k_B T}$. Generally, the energy spectrum can be divided into continuum and bound parts, yielding [27]

$$\begin{aligned}
b_{1,1} &= 2\sqrt{2}\frac{\lambda^3_{m_1}}{\lambda^3_{M/2}}\left[\sum_b\exp\left(\frac{-\varepsilon_b}{k_B T}\right) + \frac{\lambda^2_{m_r}}{2\pi^2}\sum_l(2l+1)\right. \\
&\quad\left.\times\int_0^\infty\exp\left(\frac{-\hbar^2k^2}{2m_r k_B T}\right)\delta_l(k)kdk\right],
\end{aligned} \tag{16}$$

where $\lambda_{m_r} = h/\sqrt{\pi m_r k_B T}$. ε_b is the energy of the bound state, l the partial wave, and $\delta_l(k)$ the phase shift.

B. Third virial coefficients

In this section, we derive the virial coefficients related to the three-particle interaction along the lines of Beth and Uhlenbeck's work by using the Lee-Yang binary collision theory. We consider the s-wave interaction between distinguishable species. High-order partial waves with $l > 0$ are neglected since their background scattering phase shift is several orders of magnitude smaller than that of the s wave.

To calculate the virial coefficients b_{N_1,N_2} $(N_1 + N_2 > 2)$ using Lee-Yang theory, we treat separately the interaction $u(r_{i,j})$ and the quantum statistical effect resulting from the symmetry of the wave function [21]. First, we introduce a Boltzmann system with an asymmetric wave function, and then define corresponding operators W_{N_1,N_2} and U_{N_1,N_2} in the same way as in Eq. (7). The relationship between W_{N_1,N_2} and $W^{\mathrm{FD}}_{N_1,N_2}$ is given by

$$\begin{aligned}&\langle 1',\ldots,(N_1+N_2)'|W^{\mathrm{FD}}_{N_1,N_2}|1,\ldots,(N_1+N_2)\rangle\\&\quad=\sum_{P'}\epsilon_{P'}P'\langle 1',\ldots,(N_1+N_2)'|W_{N_1,N_2}|1,\ldots,(N_1+N_2)\rangle,\end{aligned}\tag{17}$$

where P' is any one of the $N_1!N_2!$ operators which permute the variables $1',2',\ldots,(N_1+N_2)'$. $\epsilon_{P'} = +1$ (-1) if the permutation of the normal order is even (odd). Thus we can express $U^{\mathrm{FD}}_{N_1,N_2}$ in terms of U_{N_1,N_2} as

$$\begin{aligned}\langle 1',2',3'|U^{\mathrm{FD}}_{2,1}|1,2,3\rangle &= \langle 1',2',3'|U_{2,1}|1,2,3\rangle\\&\quad-\langle 2',1',3'|U_{2,1}|1,2,3\rangle\\&\quad-\langle 2'|U_{1,0}|1\rangle\langle 1',3'|U_{1,1}|2,3\rangle\\&\quad-\langle 1'|U_{1,0}|2\rangle\langle 2',3'|U_{1,1}|1,3\rangle.\end{aligned}\tag{18}$$

Similarly, we can get the matrix elements of $U^{\mathrm{FD}}_{1,2}$. The expression for $b_{2,1}$ is given by

$$\begin{aligned}b_{2,1} &= \frac{\lambda^3_{m_1}}{2V}\mathrm{Tr}\big(U^{\mathrm{FD}}_{2,1}\big)\\&=\frac{\lambda^3_{m_1}}{2V}\mathrm{Tr}\{\langle 1,2,3|U_{2,1}|1,2,3\rangle-\langle 2,1,3|U_{2,1}|1,2,3\rangle\\&\quad-\langle 2|U_{1,0}|1\rangle\langle 1,3|U_{1,1}|2,3\rangle\\&\quad-\langle 1|U_{1,0}|2\rangle\langle 2,3|U_{1,1}|1,3\rangle\}\end{aligned}\tag{19}$$

and $b_{1,2}$ can be easily deduced by exchanging the coordinates between species γ_1 and γ_2. The last two terms in the braces of Eq. (19) give the same contributions to $b_{2,1}$ since $|1\rangle$ and $|2\rangle$ are the coordinates of indistinguishable particles, and hence Eq. (19) can be reduced to

$$\begin{aligned}b_{2,1} &= \frac{\lambda^3_{m_1}}{2V}\mathrm{Tr}\{\langle 1,2,3|U_{2,1}|1,2,3\rangle-\langle 2,1,3|U_{2,1}|1,2,3\rangle\}\\&\quad-\frac{\lambda^3_{m_1}}{V}\mathrm{Tr}\{\langle 1|U_{1,0}|2\rangle\langle 2,3|U_{1,1}|1,3\rangle\}.\end{aligned}\tag{20}$$

By introducing $\mathbf{R} = (m_1\mathbf{r}_2 + m_2\mathbf{r}_3)/m_1m_2$, $\mathbf{R}' = (m_1\mathbf{r}_1 + m_2\mathbf{r}_3)/m_1m_2$, $\mathbf{r} = \mathbf{r}_2 - \mathbf{r}_3$, and $\mathbf{r}' = \mathbf{r}_1 - \mathbf{r}_3$, the matrix elements of the last term in Eq. (20) are expressed as

$$\begin{aligned}\langle 1|U_{1,0}|2\rangle &= \frac{1}{\lambda^3_{m_1}}\exp\left[-\frac{(\mathbf{r}_1-\mathbf{r}_2)^2m_1k_BT}{2}\right]\\&=\frac{1}{\lambda^3_{m_1}}\exp\left[-\frac{(\mathbf{r}-\mathbf{r}')^2m_1k_BT}{2}\right],\end{aligned}\tag{21}$$

$$\begin{aligned}&\langle 2,3|U_{1,1}|1,3\rangle\\&=\frac{V}{\lambda^3_{M/2}}\exp\left[-\frac{(\mathbf{R}-\mathbf{R}')^2(m_1+m_2)k_BT}{2}\right]\langle\mathbf{r}|u|\mathbf{r}'\rangle\\&=\frac{V}{\lambda^3_{M/2}}\exp\left[-\frac{(\mathbf{r}-\mathbf{r}')^2k_BT}{2}\left(\frac{m_1^2}{m_1+m_2}\right)\right]\langle\mathbf{r}|u|\mathbf{r}'\rangle.\end{aligned}\tag{22}$$

The relative motion part $\langle\mathbf{r}|u|\mathbf{r}'\rangle$ is given by [21]

$$\begin{aligned}\langle\mathbf{r}|u|\mathbf{r}'\rangle &= (2\pi^2rr')^{-1}P_0(\cos\theta)\\&\quad\times\left\{\frac{1}{2}\pi\sum_b R_b(r)R_b'(r')\exp\left(\frac{\varepsilon_b}{k_BT}\right)\right.\\&\quad+\int_0^\infty dk\exp\left(-\frac{\hbar^2k^2}{2m_rk_BT}\right)\\&\quad\left.\times[R_k(r)R_k(r')-R_k^0(r)R_k^0(r')]\right\},\end{aligned}\tag{23}$$

where $P_0(\cos\theta)$ is the zeroth Legendre polynomial and $\cos\theta = (rr')^{-1}\mathbf{r}\cdot\mathbf{r}'$. R_b is the wave function of the possible bound state. R_k and R_k^0 denote the continuum wave functions with and without interaction, respectively, for the two-body system. The continuum functions at $r\to\infty$ are given by

$$R_k \to \sin[kr + \delta(k)],\tag{24}$$

$$R_k^0 \to \sin(kr).\tag{25}$$

By using Eqs. (21)–(25), the last term in Eq. (20) can be expressed as

$$\begin{aligned}&\frac{\lambda^3_{m_1}}{V}\mathrm{Tr}\{\langle 1|U_{1,0}|2\rangle\langle 2,3|U_{1,1}|1,3\rangle\}\\&=\frac{1}{\lambda^3_{M/2}}\iint d\mathbf{r}d\mathbf{r}'\langle\mathbf{r}|u|\mathbf{r}'\rangle\\&\quad\times\exp\left[-\frac{(\mathbf{r}-\mathbf{r}')^2k_BT}{2}\left(\frac{m_1^2}{m_1+m_2}+m_1\right)\right].\end{aligned}\tag{26}$$

For convenience, we define $\frac{m_1^2}{m_1+m_2} + m_1 = A$, and then integrate over the angles $\mathbf{r}$ and $\mathbf{r}'$, yielding

$$\begin{aligned}&\frac{\lambda^3_{m_1}}{V}\mathrm{Tr}\{\langle 1|U_{1,0}|2\rangle\langle 2,3|U_{1,1}|1,3\rangle\}\\&=\frac{2}{\lambda^3_{m/2}}\frac{1}{A}\int_0^\infty\int_0^\infty drdr'\left\{\exp\left[-\frac{A(r-r')^2k_BT}{2}\right]\right.\end{aligned}$$

$$- \exp\left[-\frac{A(r+r')^2 k_B T}{2}\right]\Bigg\}\Bigg\{\frac{\pi}{2}\sum_b R_n(r)R_n'(r') \times \exp\left(\frac{\varepsilon_b}{k_B T}\right) + \int_0^\infty dk \exp\left(-\frac{\hbar^2 k^2}{2m_r k_B T}\right)\eta(k,r,r')\Bigg\}, \tag{27}$$

where

$$\eta(k,r,r') = R_k(r)R_k(r') - R_k^0(r)R_k^0(r'). \tag{28}$$

We treat $\eta(k,r,r')$ as did Pais *et al.* [28],

$$\eta = \eta_{\text{out}} + \eta_{\text{in}}, \tag{29}$$

$$\eta_{\text{out}} = R_k^{as}(r)R_k^{as}(r') - R_k^0(r)R_k^0(r'), \tag{30}$$

$$\eta_{\text{in}} = R_k(r)R_k(r') - R_k^{as}(r)R_k^{as}(r'), \tag{31}$$

with $R_k^{as}(r) = \sin(kr+\delta)$. Accordingly,

$$\eta_{\text{out}}(k,r,r') = \frac{\cos k(r+r') + \cot\delta \sin k(r+r')}{1+\cot^2\delta}. \tag{32}$$

In the vicinity of a Feshbach resonance, we use the expression for the phase shift [17,21]

$$k\cot\delta = -\frac{1}{a} + \frac{1}{2}r_0 k^2, \tag{33}$$

where a is the scattering length and $r_0 = (\mu C_6/8\hbar^2)^{1/4}$ an effective range with C_6 being the van der Waals coefficient. For a heavy atomic collision system with a large C_6, the contribution from r_0 to the phase shift is important near the resonance especially at high temperature. Compared with the second virial coefficient, the third virial coefficient is more senstive to r_0. Therefore ignoring any terms will cause an error in the calculation of Eq. (32). Substituting Eqs. (32) and (33) into Eq. (27), we can calculate the contribution of η_{out} to $b_{2,1}$. As the integrand of Eq. (27) is symmetrical in r and r', we may write the the contribution from η_{in} as

$$\frac{2}{\lambda_{M/2}^3}\frac{1}{A}\int_0^\infty\int_0^\infty dr dr'\Bigg\{\exp\left[-\frac{A(r-r')^2 k_B T}{2}\right] - \exp\left[-\frac{A(r+r')^2 k_B T}{2}\right]\Bigg\}\int_0^\infty dk \exp\left(-\frac{\hbar^2 k^2}{2m_r k_B T}\right) \times \left[R_k(r) + R_k^{as}(r)\right]\left[R_k(r') - R_k^{as}(r')\right]. \tag{34}$$

Furthermore, we take $R_k(r') - R_k^{as}(r') \simeq k\phi(r')$ instead of calculating the k-dependent $R_k(r)$ and obtain the contribution of η_{in} to $b_{2,1}$.

We now calculate the first term in Eq. (27) using the binary expansion method. Lee and Yang proposed a binary expansion procedure using a graph representation. We calculate $b_{2,1}$ following the prescription developed by Pais *et al.* based on the classical Ursell graph theory [28], yielding

$$U_{2,1}^c = \exp\left(-\frac{\sum_{n=1}^3 T_n}{k_B T}\right)(f_{12}f_{23} + f_{23}f_{31} + f_{31}f_{12} + f_{12}f_{23}f_{31}), \tag{35}$$

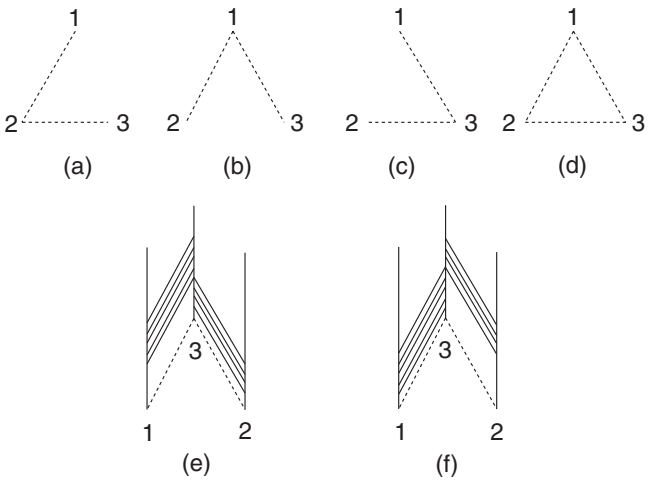

FIG. 1. (a)–(d) Classical Ursell graphs for $N_1 + N_2 = 3$. (e),(f) Two examples of connected quantum graphs corresponding to (c).

where T_n is the kinetic energies of the nth particle and $f_{ij} = \exp(-u_{ij}/k_B T) - 1$. In Figs. 1(a)–1(d), we display the classical Ursell graphs for $U_{2,1}^c$.

In the quantum statistics, $U_{2,1}$ can be expressed as a sum of four operators corresponding to Fig. 1. Taking Fig. 1(c) for example, we draw two graphs, as shown in Figs. 1(e) and 1(f). There are two planes perpendicular to the plane 1-2-3 in Figs. 1(e) and 1(f), where the shaded areas are called "blocks." A graph having at least one block in each plane will be called a connected quantum graph. The block is started from the bottom and increases alternately in the two planes. The number of blocks, N_b, can be ∞ but we neglect the contributions of $N_b > 3$. Thus every graph in Figs. 1(a)–1(c) corresponds to two connected quantum graphs. For the graph in Fig. 1(d), there are three planes and at least three blocks which are neglected in our theoretical treatment. We introduce an operator associated with the kth block in the i-j plane,

$$C(\beta_k; i, j) = B(\beta_k; i, j)\exp\left(-\beta_k \sum_{n\neq i,j} T_n\right), \tag{36}$$

where $B(\beta_k; i, j) = -u_{ij}\exp[-\beta_k(T_1 + T_2 + u_{ij})]$ is the binary operator and β_k is a parameter. In the sequence of blocks from bottom to top of a given connected quantum graph, we construct an operator of the products of C from the right to the left,

$$\hat{C}(i_1 i_2, j_1 j_2) = \int_0^\beta d\beta_1 \int_0^{\beta_1} d\beta_2 \exp\left[-(\beta - \beta_1 - \beta_2)\sum_{n=1}^3 T_n\right] \times C(\beta_2; i_2 j_2)C(\beta_1; i_1 j_1). \tag{37}$$

We then consider the contribution from $\langle 1,2,3|U_{2,1}|1,2,3\rangle$ in Eq. (27). From the general prescription for constructing connected quantum graphs, the matrix elements of $U_{2,1}$ include six graphs of the type of Fig. 1(e). By neglecting the contributions of $l > 0$ for fermions, we need only consider the contributions of Figs. 1(e) and 1(f). Thus the contribution to

$b_{2,1}$ in the momentum space can be written as

$$\frac{\lambda_{m_1}^3}{V}\int d\mathbf{q}_1 d\mathbf{q}_2 d\mathbf{q}_3 \exp\left(-\frac{T_1+T_2+T_3}{k_BT}\right) \times \iint d\beta_1 d\beta_2 \exp[\beta_1(T_2+T_3)+\beta_2(T_1+T_3)] \times \langle \mathbf{q}_1,\mathbf{q}_3|B(\beta_2)|\mathbf{q}_1,\mathbf{q}_3\rangle\langle \mathbf{q}_2,\mathbf{q}_3|B(\beta_1)|\mathbf{q}_2,\mathbf{q}_3\rangle, \quad (38)$$

where $\beta_1+\beta_2 \leqslant \beta$. In the s-wave approximation, the contribution from $\langle 2,1,3|U_{2,1}|1,2,3\rangle$ give the same value as that from $\langle 1,2,3|U_{2,1}|1,2,3\rangle$. Based on the above analysis, we can see that the first term in Eq. (27) gives no contribution to the virial coefficient.

C. The interaction energy in terms of virial coefficients

By using the relation $\Omega = PV$, the pressure can be expanded as

$$P = P_0 + \frac{k_BT}{\lambda_{m_1}^3}\left(b_{2,0}z_1^2 + b_{0,2}z_2^2 + b_{1,1}z_1z_2 + b_{3,0}z_1^3 + b_{0,3}z_2^3 + b_{2,1}z_1^2z_2 + b_{1,2}z_1z_2^2\right), \quad (39)$$

where P_0 is the pressure of a weakly degenerate ideal Fermi gas. The fugacity expansion of P_0 up to the third order can be written as

$$P_0 = \frac{k_BT}{\lambda_{m_1}^3}\left(z_1 - 2^{-5/2}z_1^2 + 3^{-5/2}z_1^3\right) + \frac{k_BT}{\lambda_{m_2}^3}\left(z_2 - 2^{-5/2}z_2^2 + 3^{-5/2}z_2^3\right). \quad (40)$$

Neglecting the contribution of $l > 0$, we can simplify Eq. (39) as

$$P = P_0 + \frac{k_BT}{\lambda_{m_1}^3}\left(b_{1,1}z_1z_2 + b_{2,1}z_1^2z_2 + b_{1,2}z_1z_2^2\right). \quad (41)$$

Using the relations $dP = \sum_i n_i d\mu_i + sdT$ and $\epsilon = Ts + \sum_i n_i\mu_i - P$, we obtain the number density n_i of species γ_i, the entropy density s, and the energy density ϵ as follows:

$$n_1 = \frac{1}{\lambda_{m_1}^3}\left(z_1 - 2^{-3/2}z_1^2 + 3^{-3/2}z_1^3\right) + \frac{1}{\lambda_{m_1}^3}\left(b_{1,1}z_1z_2 + 2b_{2,1}z_1^2z_2 + b_{1,2}z_1z_2^2\right), \quad (42a)$$

$$n_2 = \frac{1}{\lambda_{m_2}^3}\left(z_2 - 2^{-3/2}z_2^2 + 3^{-3/2}z_2^3\right) + \frac{1}{\lambda_{m_1}^3}\left(b_{1,1}z_1z_2 + b_{2,1}z_1^2z_2 + 2b_{1,2}z_1z_2^2\right), \quad (42b)$$

$$s = \frac{5P}{2T} - \frac{\mu_1n_1+\mu_2n_2}{T} + \frac{k_BT}{\lambda_{m_1}^3}\left(\frac{\partial b_{1,1}}{\partial T}z_1z_2 + \frac{\partial b_{2,1}}{\partial T}z_1^2z_2 + \frac{\partial b_{1,2}}{\partial T}z_1z_2^2\right), \quad (42c)$$

$$\epsilon = \frac{3P}{2} + \frac{k_BT}{\lambda_{m_1}^3}\left(T\frac{\partial b_{1,1}}{\partial T}z_1z_2 + T\frac{\partial b_{2,1}}{\partial T}z_1^2z_2 + T\frac{\partial b_{1,2}}{\partial T}z_1z_2^2\right) = \epsilon_{\rm kin} + \epsilon_{\rm int}, \quad (42d)$$

where $\epsilon_{\rm kin}$ and $\epsilon_{\rm int}$ are the kinetic and interaction energy densities, respectively. Generally, the temperature of an ultracold gas does not change when the system crosses a Feshbach resonance. Jo *et al.* found experimentally that when the ultracold gas approaches the resonance from the repulsive side, it expands, which lowers the gas density and Fermi energy [29]. At the phase transition, the kinetic energy increases and the interaction energy decreases. They also pointed out that the measured kinetic energy may include some interaction energy. Here, we assume the total number density remains unchanged and the kinetic energy is a constant in the system evolution process.

It is straightforward to show that

$$z_1 = n_1\lambda_{m_1}^3 + 2^{-3/2}z_1^2 - 3^{-3/2}z_1^3 - b_{1,1}z_1z_2 - 2b_{2,1}z_1^2z_2 - b_{1,2}z_1z_2^2, \quad (43)$$

$$z_2 = n_2\lambda_{m_2}^3 + 2^{-3/2}z_2^2 - 3^{-3/2}z_2^3 - \left(\frac{m_2}{m_1}\right)^{3/2}\left(b_{1,1}z_1z_2 - 2b_{2,1}z_1^2z_2 - b_{1,2}z_1z_2^2\right). \quad (44)$$

Then we extract the terms that are independent of the virial coefficients from the expressions for the fugacity up to the third order,

$$z_1^2 = \left(n_1\lambda_{m_1}^3\right)^2 + 2^{-1/2}\left(n_1\lambda_{m_1}^3\right)^3 + \cdots, \quad (45a)$$

$$z_2^2 = \left(n_2\lambda_{m_2}^3\right)^2 + 2^{-1/2}\left(n_2\lambda_{m_2}^3\right)^3 + \cdots, \quad (45b)$$

$$z_1^3 = \left(n_1\lambda_{m_1}^3\right)^3 + \cdots, \quad (45c)$$

$$z_2^3 = \left(n_2\lambda_{m_2}^3\right)^3 + \cdots, \quad (45d)$$

$$z_1 = n_1\lambda_{m_1}^3 + 2^{-3/2}\left(n_1\lambda_{m_1}^3\right)^2 + 2^{-2}\left(n_1\lambda_{m_1}^3\right)^3 - 3^{-3/2}\left(n_1\lambda_{m_1}^3\right)^3 + \cdots, \quad (45e)$$

$$z_2 = n_2\lambda_{m_2}^3 + 2^{-3/2}\left(n_2\lambda_{m_2}^3\right)^2 + 2^{-2}\left(n_2\lambda_{m_2}^3\right)^3 - 3^{-3/2}\left(n_2\lambda_{m_2}^3\right)^3 + \cdots. \quad (45f)$$

Substituting Eq. (45) into the expression for the energy density in Eq. (42) and eliminating all the terms related to virial coefficients, we can obtain the kinetic energy density $\epsilon_{\rm kin}$ and the interaction energy density $\epsilon_{\rm int} = \epsilon - \epsilon_{\rm kin}$.

III. RESULTS AND DISCUSSION

We first study the virial coefficients in the vicinity of a Feshbach resonance. The mixture of ^{6}Li and ^{40}K, as the prime candidate for studying a strongly Fermi-Fermi interacting system, is very popular in experiments. Wille *et al.* and Kohstall *et al.* identified the most of Feshbach resonances in ^{6}Li-^{40}K mixtures [5] and investigated the broad resonance centered at $B_0 = 154.719$ G for the spin states $F_{\rm Li} = 1/2$, $m_{F_{\rm Li}} = 1/2$, $F_{\rm K} = 9/2$, and $m_{F_{\rm K}} = -5/2$ at temperature $T = 290$ nK [10]. Here we consider the thermodynamics of the ^{6}Li-^{40}K mixture near the resonance at 154.719 G at higher temperature using the virial expansion theory. Figure 2 shows the virial coefficients as a function of magnetic field at different temperatures. The magnitude of the virial coefficients depends on the mass ratio m_2/m_1. In

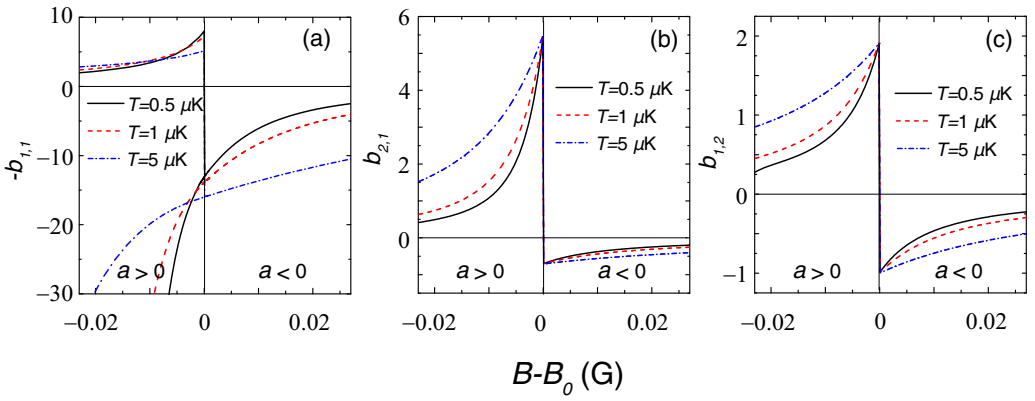

FIG. 2. (Color online) The virial coefficients as a function of magnetic field at different temperatures.

Fig. 2(a), $-b_{11}$ displays two *branches* [17]. When the system approaches the resonance from the $B - B_0 > 0$ side where $a < 0$, $-b_{1,1} < 0$ and decreases rapidly when the system evolves to the $B - B_0 < 0$ side where $a > 0$. However, if the system approaches the resonance from the $B - B_0 < 0$ side, $-b_{1,1} > 0$ and increases with increasing magnetic field. At the resonance, $-b_{1,1}$ jumps to a negative value, and then evolves along the low branch. Unlike $-b_{1,1}$, $b_{2,1}$ and $b_{1,2}$ have

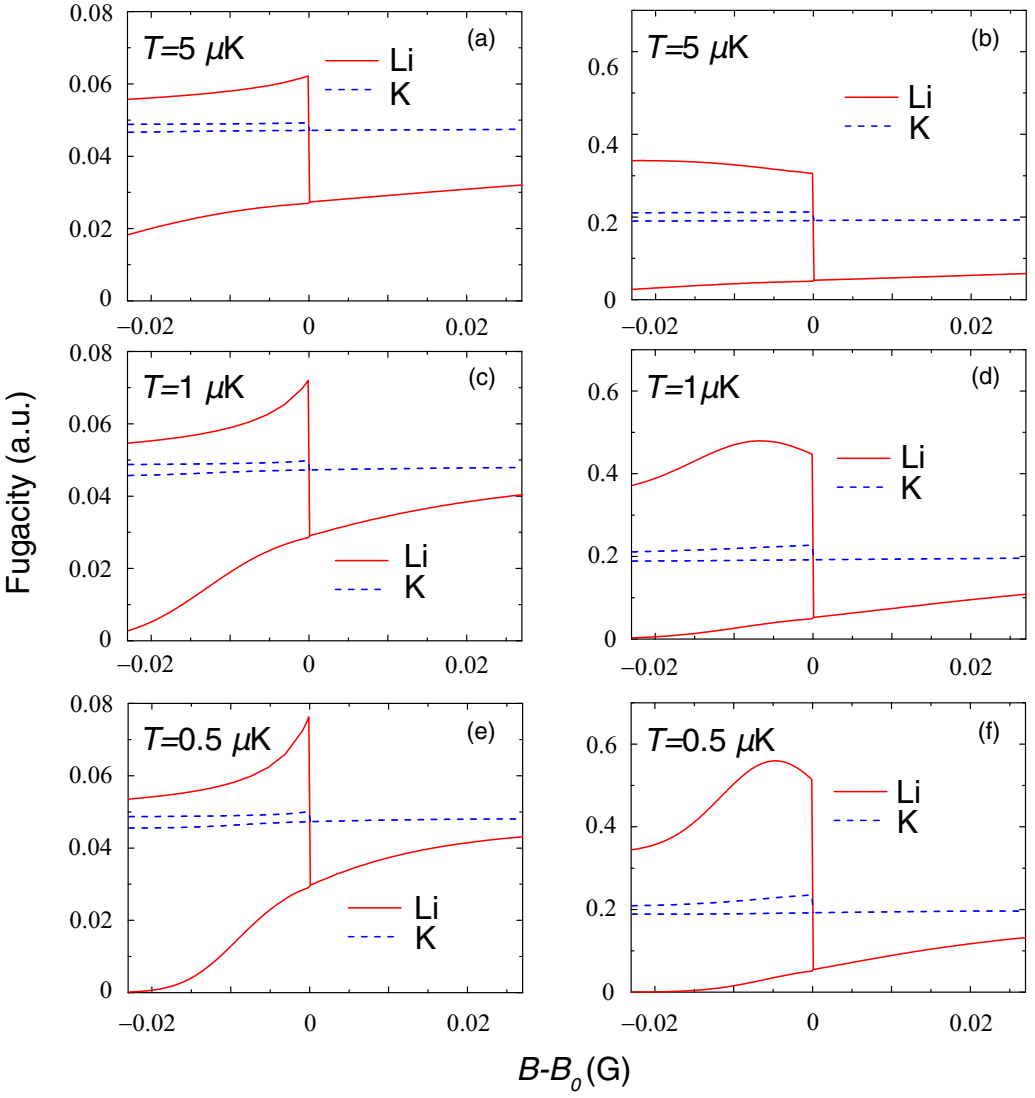

FIG. 3. (Color online) The fugacities of two species versus magnetic field at different temperatures. In (a), (c), and (e) $T/T_F = 10$. In (b), (d), and (f) $T/T_F = 4$.

only one branch, because the contribution of the two-body bound state to the third virial coefficient is very small near the resonance at high temperature, which means that the formation or disassociation of the two-body bound pair has little effect on the many-body interaction. Far from the resonance or at the low-temperature limit, we can observe two branches in Figs. 2(b) and 2(c).

In Ho and Mueller's work, the fugacity is eliminated and its value is replaced by the parameter $n\lambda^3$ in the interaction energy density equation [17]. However, $-b_{1,1}$ decreases rapidly in the low branch, as shown in Fig. 2(a), since the bound state becomes deeper with decrease of magnetic field. In this case, we cannot describe the fugacity by a constant in the high-order terms. Figure 3 shows the fugacities as a function of magnetic field at different temperatures. To simplify the discussion, we define the Fermi temperature of the system as T_F and consider only $T_{F_{\rm Li}} = T_{F_{\rm K}} = T_F$. The curves in Figs. 3(a), 3(c), and 3(e) exhibit variation trends similar to those of the second virial coefficient in Fig. 2(a) with varying magnetic field, because the lower fugacity is mainly governed by the second-order interaction. When the system crosses the resonance, the fugacity of the light species undergoes a great change at lower temperature (T/T_F unchanged). The fugacity of the heavy species is not sensitive to temperature for the same T/T_F due to the large mass ratio ($m_{\rm K}/m_{\rm Li} \approx 6.67$). At the same T but different T_F, we find that the magnitude of the fugacity increases with increase of T_F. According to $n\lambda^3 = (8/3\sqrt{\pi})(T_F/T)^{3/2}$, the number density of species is inversely proportional to $(T/T_F)^{3/2}$; the decrease of T_F/T causes the number density to increase and the fugacity to enlarge. At lower temperature, the fugacity gets closer to 1 and more high-order terms in the virial expansion should be considered. If $z_i \gg 1$, the contributions from high-order terms are far larger than those from low-order terms and hence the virial expansion is invalid. Additionally, $z_{\rm Li}$ in the upper branch does not monotonically change with magnetic field when T/T_F decreases, and the position of the maximum shifts to the left with increasing temperature. By fixing T/T_F, the

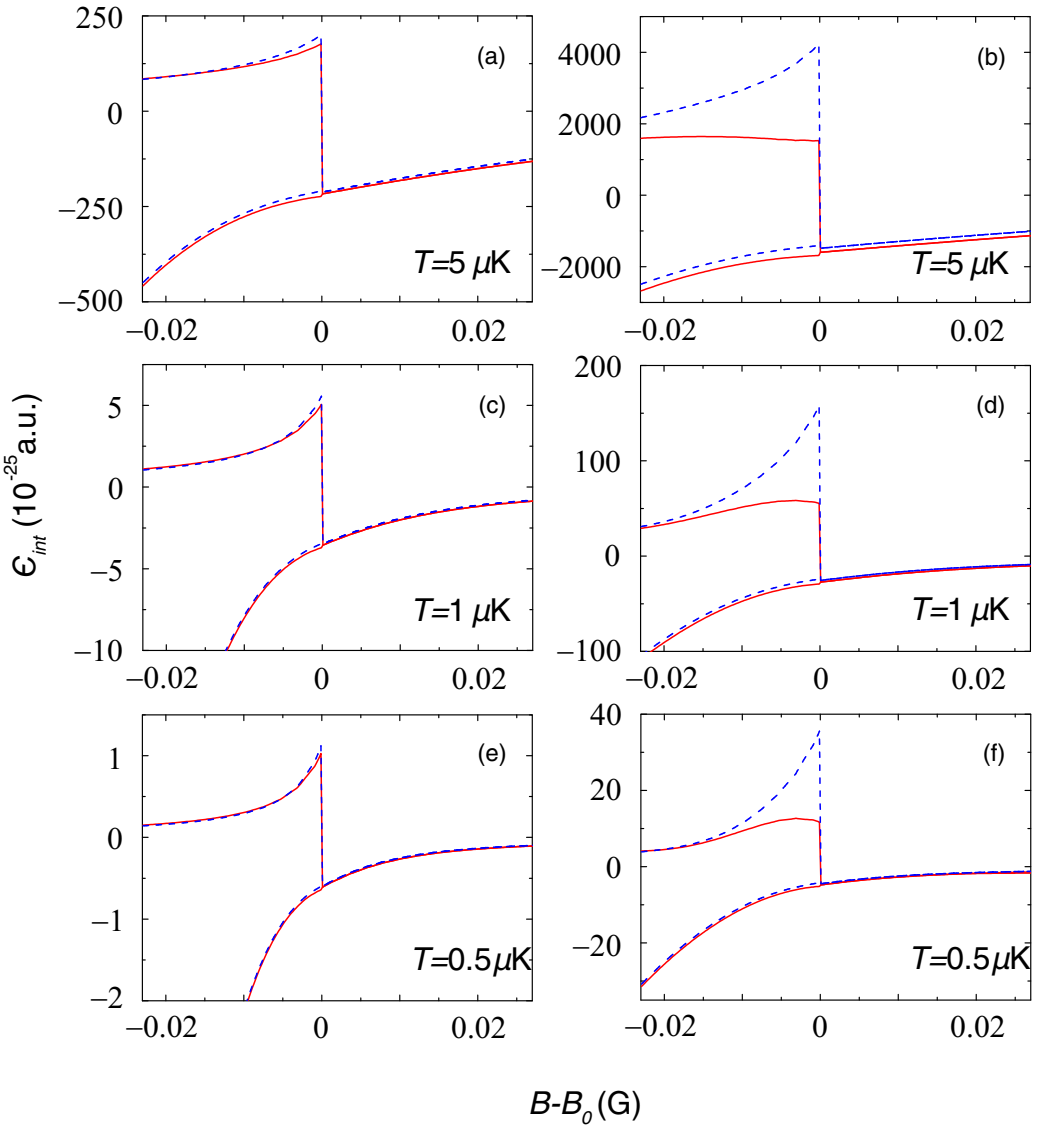

FIG. 4. (Color online) The interaction energy densities versus the magnetic field at different temperatures corresponding to Figs. 3(a)–3(f). The blue dashed and red solid lines represent the results using the virial expansion up to second and third orders, respectively.

maximum in the upper branch comes closer to the resonant position with decreasing temperature. Recently, Jo *et al.* measured the chemical potential at lower temperature on the repulsive side. Our calculation exhibits a similar behavior to their result [29].

The magnitude of the nth virial coefficient in Eq. (42d) represents the n-body interaction strength, and the interaction energy is related to the density of the gas. Since the magnitude of the third virial coefficient is nearly the same as that of the second virial coefficient near the resonance, the many-body interaction cannot be ignored when the gas is not rare enough at microkelvin temperatures. The scattering length is related to the two-body interaction. However, it cannot be used to explain the many-body effect observed in experiments [3,29]. Here we calculate the interaction energy density in order to describe the quantum many-body effect using the virial expansion method. To discuss the contribution of the third-order terms, we show the interaction energy densities as a function of magnetic field using the virial expansion up to the second and third orders in Fig. 4. The calculated results using the virial expansion up to the second order exhibit a good convergence at $T/T_F = 10$. However, an obvious discrepancy between two curves in the upper branch occurs at $T/T_F = 4$, because the contribution of high-order terms is directly related to the magnitude of the fugacity. By keeping T unchanged, with a decrease of T/T_F, the number density and $\epsilon_{\rm int}$ increase. Moreover, the position of the maximal $\epsilon_{\rm int}$ in the upper branch shifts to the left at $T/T_F = 4$, similarly to the variation trend of $z_{\rm Li}$. Bourdel *et al.* observed similar behavior and negative interaction energy on the repulsive side at $T = 5.25\ \mu$K [3]. We calculate the interaction energy density at smaller T/T_F and also find negative interaction energy on the repulsive side. However, the fugacity easily exceeds 0.7. In this case, the error from high-order terms may be tremendous (the result is not shown here). Since this feature cannot be found in the calculation of the second-order virial expansion, it should arise from many-body interactions. Shenoy *et al.* pointed out that this phenomenon results from Pauli blocking which causes the bound states of fermion pairs with different momenta to disappear at different scattering lengths [30]. In our work, we cannot draw the conclusion that this feature is caused by Pauli blocking. We are sure that the three-body interaction will reduce the interaction energy since the third-order and second-order virial coefficients possess opposite signs. By introducing higher-order virial coefficients, we may find more interesting phenomena at low temperature.

We now consider the case of $T_{F_{\rm Li}} \neq T_{F_{\rm K}}$. Figure 5 shows the fugacities as a function of magnetic field at different $T_{F_{\rm Li}}$ but fixed $T_{F_{\rm K}}$. The magnitude of $z_{\rm Li}$ decreases with decreasing $T_{F_{\rm Li}}$ due to the decrease of the number density, while the magnitude of $z_{\rm K}$ almost remains unchanged. In this case, the magnitudes of the fugacities of the two species are mainly determined by the number density. We also calculate the fugacities at different $T_{F_{\rm K}}$ but fixed $T_{F_{\rm Li}}$, and find that the magnitude of $z_{\rm K}$ decreases with decreasing $T_{F_{\rm K}}$ but the magnitude of $z_{\rm Li}$ changes irregularly. This means that the fugacity of the heavy species is mostly determined by the number density. If $m_2/m_1 \to \infty$, the fugacity of the heavy species will be entirely determined by the number density since the interaction energy between particles can be neglected compared with the kinetic energy.

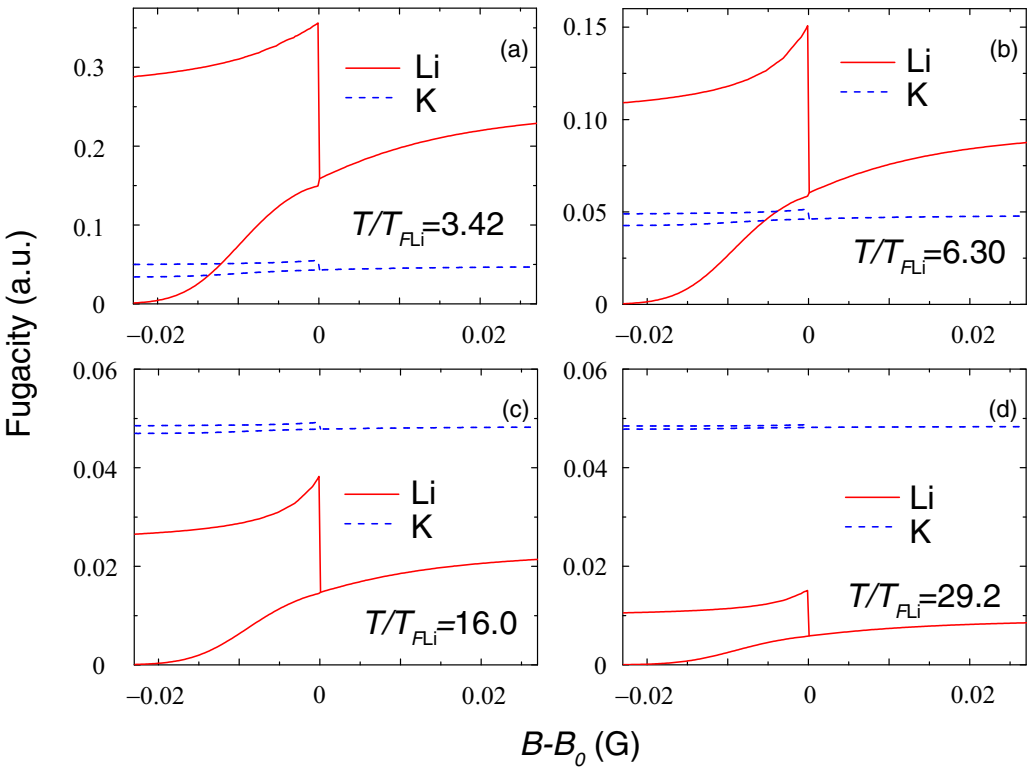

FIG. 5. (Color online) Fugacities as a function of magnetic field at $T = 0.5\ \mu$K and $T_{F_K} = 0.05\ \mu$K.

IV. CONCLUSION

We have studied theoretically the thermodynamics of mixed ^{6}Li-^{40}K Fermi gases around the s-wave Feshbach resonance using the virial expansion method. The magnitude of the virial coefficient depends on the mass ratio of the two species. The contribution of the two-body bound state to high-order virial coefficients can be neglected compared with that of the scattering continuum state near the Feshbach resonance at microkelvin temperatures. At the resonance, the fugacity of the light atoms undergoes a sharp change while that of the heavy atoms changes slightly when $T_{F_{\rm Li}} = T_{F_{\rm K}}$. The positions of the maxima of the fugacity and interaction energy density in the upper branch shift to the left with decrease of T/T_F due to three-body interactions. The relevance between the fugacity of the heavy species and the number density depends on the mass ratio. Compared with the work of Liu *et al*. [22], our theory is applicable to an arbitrary interaction regime and can be used to explore the quantum many-body effect at ultralow temperature. By introducing more high-order virial coefficients, we may find other interesting phenomena in mass-imbalanced Fermi gases at low temperature.

ACKNOWLEDGMENTS

This work is supported by the National Natural Science Foundation of China under Grants No. 10974024 and No. 11274056.

[1] C. Chin, R. Grimm, P. S. Julienne, and E. Tiesinga, Rev. Mod. Phys. **82**, 1225 (2010).
[2] K. M. O'Hara, S. L. Hemmer, M. E. Gehm, S. R. Granade, and J. E. Thomas, Science **298**, 2179 (2002).
[3] T. Bourdel, J. Cubizolles, L. Khaykovich, K. M. F. Magalhães, S. J. J. M. F. Kokkelmans, G. V. Shlyapnikov, and C. Salomon, Phys. Rev. Lett. **91**, 020402 (2003).
[4] E. L. Hazlett, Y. Zhang, R. W. Stites, and K. M. O'Hara, Phys. Rev. Lett. **108**, 045304 (2012).
[5] E. Wille, F. M. Spiegelhalder, G. Kerner, D. Naik, A. Trenkwalder, G. Hendl, F. Schreck, R. Grimm, T. G. Tiecke, J. T. M. Walraven, S. J. J. M. F. Kokkelmans, E. Tiesinga, and P. S. Julienne, Phys. Rev. Lett. **100**, 053201 (2008).
[6] A.-C. Voigt, M. Taglieber, L. Costa, T. Aoki, W. Wieser, T. W. Hänsch, and K. Dieckmann, Phys. Rev. Lett. **102**, 020405 (2009).
[7] F. M. Spiegelhalder, A. Trenkwalder, D. Naik, G. Hendl, and F. Schreck, and R. Grimm, Phys. Rev. Lett. **103**, 223203 (2009).
[8] P. S. Żuchowski, J. Aldegunde, and J. M. Hutson, Phys. Rev. Lett. **105**, 153201 (2010)
[9] H.-W. Cho, D. J. McCarron, M. P. Köppinger, D. L. Jenkin, K. L. Butler, P. S. Julienne, C. L. Blackley, C. R. Le Sueur, J. M. Hutson and S. L. Cornish, Phys. Rev. A **87**, 010703(R) (2013).
[10] C. Kohstall, M. Zaccanti, M. Jag, A. Trenkwalder, P. Massignan, G. M. Bruun, F. Schreck, and R. Grimm, Nature (London) **485**, 615 (2012).
[11] W. V. Liu and F. Wilczek, Phys. Rev. Lett. **90**, 047002 (2003).
[12] D. S. Petrov, C. Salomon, and G. V. Shlyapnikov, J. Phys. B **38**, S645 (2005).
[13] P. Massignan and G. M. Bruun, Eur. Phys. J. D **65**, 83 (2011).
[14] P. Nozieres and S. Schmitt-Rink, J. Low Temp. Phys. **59**, 195 (1985).
[15] D. B. Kaplan and S. C. Sun, Phys. Rev. Lett. **107**, 030601 (2011).
[16] X. J. Liu, H. Hu, and P. D. Drummond, Phys. Rev. Lett. **102**, 160401 (2009).
[17] T. L. Ho and E. J. Mueller, Phys. Rev. Lett. **92**, 160404 (2004).
[18] K. M. Daily and D. Blume, Phys. Rev. A **85**, 013609 (2012).
[19] Z. H. Lan, G. M. Bruun, and C. Lobo, Phys. Rev. Lett. **111**, 145301 (2013).
[20] E. Beth and G. K. Uhlenbeck, Physica (Utrecht) **3**, 729 (1936).
[21] T. D. Lee and C. N. Yang, Phys. Rev. **113**, 1165 (1959).
[22] X. J. Liu and H. Hu, Phys. Rev. A **82**, 043626 (2010).
[23] J. E. Mayer, J. Chem. Phys. **5**, 67 (1937).
[24] J. E. Mayer and P. G. Ackermann, J. Chem. Phys. **5**, 74 (1937).
[25] J. E. Mayer and S. F. Harrison, J. Chem. Phys. **6**, 87 (1938).
[26] S. F. Harrison and J. E. Mayer, J. Chem. Phys. **6**, 101 (1938).
[27] L. Groper, Phys. Rev. **50**, 963 (1936).
[28] A. Pais and G. E. Uhlenbeck, Phys. Rev. **116**, 250 (1959).
[29] G.-B. Jo, Y.-R. Lee, J.-H. Choi, C. A. Christensen, T. H. Kim, J. H. Thywissen, D. E. Pritchard, and W. Ketterle, Science **325**, 1521 (2009).
[30] V. B. Shenoy and T. L. Ho, Phys. Rev. Lett. **107**, 210401 (2011).